Title
Staging of RF-accelerating Units in a MEMS-based Ion Accelerator

Authors
Persaud, A
Seidl, PA
Ji, Q
et al.

Publication Date
2017

DOI
10.1016/j.phpro.2017.09.040

Peer reviewed

Staging of RF-accelerating units in a MEMS-based ion accelerator

A. Persaud,* P. A. Seidl, Q. Ji, E. Feinberg†, W. L. Waldron, and T. Schenkel
Accelerator Technology & Applied Physics, E. O. Lawrence Berkeley National Laboratory
1 Cyclotron Road, Berkeley CA 94720, United States

S. Ardanuc, K. B. Vinayakumar, and A. Lal
School of Electrical and Computer Engineering, Cornell University
120 Phillips Hall, Ithaca NY 14853, United States

Multiple Electrostatic Quadrupole Array Linear Accelerators (MEQALACs) provide an opportunity to realize compact radio-frequency (RF) accelerator structures that can deliver very high beam currents. MEQALACs have been previously realized with acceleration gap distances and beam aperture sizes of the order of centimeters. Through advances in Micro-Electro-Mechanical Systems (MEMS) fabrication, MEQALACs can now be scaled down to the sub-millimeter regime and batch processed on wafer substrates. In this paper, we show first results from using three RF stages in a compact MEMS-based ion accelerator. The results presented show proof-of-concept with accelerator structures formed from printed circuit boards using a 3×3 beamlet arrangement and noble gas ions at 10 keV. We present a simple model to describe the measured results. The model is then used to examine some of the aspects of this approach, such as possible effects of alignment errors. We also discuss some of the scaling behaviour of a compact MEQALAC. The MEMS-based approach enables a low-cost, highly versatile accelerator covering a wide range of beam energies and currents. Applications include ion-beam analysis, mass spectrometry, materials processing, and at very high beam powers, plasma heating.

I. INTRODUCTION

A driving force in the development of new accelerators for applications in research and industry is reducing the cost and the size of the instrument while at the same time achieving higher beam intensity. In Persaud et al. [4], we proposed a new concept to achieve high beam intensities using a very compact multi-beamlet accelerator structure. The concept is based on earlier work on Multiple Electrostatic Quadrupole Array Linear Accelerators (MEQALACs) in the 1980s by Maschke [3] and has been implemented by, for example, Urbanus et al. [7] using beamlet apertures on the order of centimeters. We propose to reduce the size by greater than an order of magnitude by implementing the MEQALAC concept using micro-electro-mechanical systems (MEMS) structures, reducing the aperture size to the (sub-) millimeter scale and possibly to the scale of tens of micrometers. The MEQALAC is based on the fact that decreasing the beam aperture size in the electrostatic quadrupoles (ESQs), which supply the needed beam focusing, leads to higher transportable beam current densities. Therefore, it is advantageous to replace a large aperture and its focusing quadrupoles with multiple small apertures and quadrupoles closely packed in the transverse plane. The smallest achievable size is determined by fabrication errors. For example, fabrication errors will lead to the displacement of quadrupole centers from the desired beamline axis, leading to beam centroid oscillations and particle loss. Using MEMS technology will push these fabrication errors into the micrometer range and therefore allow better alignment and high beam intensities. Using multiple apertures in parallel will then allow to increase the total transported beam current compared to single aperture accelerators.

The accelerator structure contains two elements: electrostatic quadrupole lenses to focus the beam and transport it along the beam line, and radio-frequency (RF) acceleration. Compared to non-RF accelerators, one of the advantages of a MEQALAC structure is the use of relatively small voltages (< 10 kV) to achieve high beam energies (up to MeV). All elements are to be implemented in a silicon wafer structure, so that they can be easily fabricated using MEMS technology. For the initial proof-of-concepts experiment, both RF and ESQ structures have been implemented in circuit boards (FR-4) using millimeter-scale structures and a 3×3 array of beamlets. The FR-4 boards are fabricated by laser cutting, see Persaud et al. [4] for details on the fabrication procedure. In this paper we will focus on experiments using two and three RF units that have been realized in FR-4. We will show results from staging these RF units and compare these measurements with a simple 1D-model.

II. EXPERIMENTAL SETUP

To demonstrate the staging of several RF units, the setup shown in Fig. 1 was used. A multi-cusp ion source driven by a filament discharge, as described in Ji et al. [1], is used to create the injected ion beam. The flow of argon gas is set to achieve a pressure of 7 mTorr inside

†Now XTD-IDA, Los Alamos National Laboratory, Los Alamos, NM 87545
*E-mail:apersaud@lbl.gov

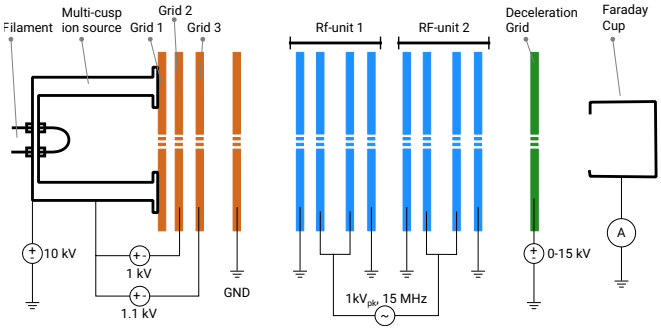

FIG. 1: The experimental setup consists of an ion source at high potential, an extraction grid system, the RF units, a retarding-potential analyzer, and a Faraday cup.

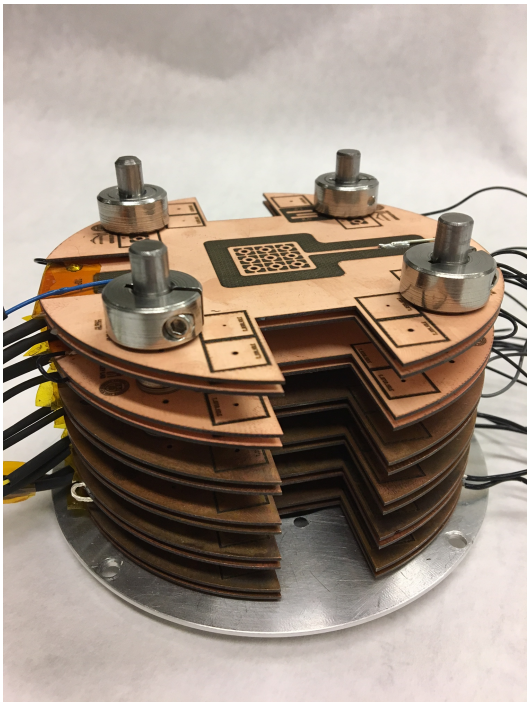

FIG. 2: Assembly of three RF units with drift spaces between the acceleration gaps set up for argon ions at 11 keV kinetic energy and an RF frequency of 15 MHz at 1 kV amplitude.

the source body. The filament operates at 3.5 V and 36 A for 7.5 seconds. After 6 seconds of filament heating an arc-pulse of -100 V is applied for 300 μs between the filament and the source housing to ignite the plasma. The ion beams (a 3×3 array with a pitch of 5 mm) are then extracted between two aligned hole plates (grids 1&2 in Fig. 1) by floating grid 1 and biasing grid 2 to -1 kV. A third hole plate (grid 3 in Fig. 1) is available at the source to enable fast beam pulsing, but this feature was not utilized in the experiments described in this paper and the plate was instead biased at a constant -1.1 kV. To be able to operate the RF and quadrupole wafers at ground potential, the ion source and the source grid power supplies are floating on high voltage (< 12 kV). This voltage will accelerate the ions to a grounded electrode that marks the end of the source setup. Afterwards the ions enter two or more RF units. A single RF unit consists of four wafers. The outer wafers are grounded and RF is applied to the inner wafers, so that for each beamlet a field between wafer 1&2 and 3&4 is created, but the region between wafer 2&3 is kept field free. Ions are accelerated or decelerated when entering the regions with electric fields. The length of the field free region can be chosen so that ions are accelerated in both gaps if they arrive at the right phase of the RF signal. For this to happen the RF needs to change sign during the time the ion drifts through the field free region. This condition is met when the drift length is $\frac{\beta\lambda}{2}$ where β is the velocity of the ion relative to the speed of light and λ is the wavelength of the RF signal. RF units can be stacked by adding another drift region between neighboring RF units. As the ions gain energy along the accelerator structure, the length of the drift regions has to increase along the beamline, see Fig. 2 for an image of an assembly of three RF units as used in the experiments. To measure the energy distribution of the ions a retarding-field grid is positioned between the exit of the last RF unit and a Faraday cup to measure the beam current. By increasing the retarding potential on the grid, ions with a lower beam energy than the applied grid voltage will be deflected and cannot enter the Faraday cup. A large opening at the Faraday cup ensures that all ions passing through the retarding grid are collected.

In our setup, we generate the RF signal from a RF-signal generator (Keysight 33500B) that gets amplified to < 1 W signal using a Mini-Circuits ZHL-2-8 and in turn drives the gate of an RF-MOSFET to excite a tuned resonator. The main RF loads are in the MOSFET circuit and from the RF wafer capacitance of the order of $\sim$ pF/gap. All RF units are connected in parallel to the same RF source in our setup. The typical pressure in the vacuum chamber is in the low 10^{-6} Torr range without gas flow and rises to 2×10^{-5} Torr when the gas flow is on. The power supplies as well as the RF generator are remote controlled via LabVIEW [2]. Furthermore, we monitor and control voltage and current signals using National Instruments cDAQ modules. A Picoscope (Picoscope 5443B) is used inside the high voltage rack that houses the grid power supplies of the source to monitor voltages and currents of the extraction system. The oscilloscope is controlled using Python [5] running on a Raspberry Pi and communicates its data to LabVIEW using ZeroMQ [8] over a fiber-coupled ethernet connection. Timing is controlled by two Stanford Research Systems DG535 modules which are connected to LabVIEW. A Tektronix Oscilloscope is used to measure the Faraday cup signal, which is measured across a 10 kΩ resistor.

A voltage scan on the retarding grid can be used to measure the energy distribution of the beam. The long beam pulse of 0.3 ms relative to the RF frequency of 15 MHz will create a continuous distribution of ion energy where some particles are accelerated and others deceler-

ated. If the drift regions are designed for the right ion species and velocities, some ions can achieve acceleration across all gaps. Other ions arriving at the wrong phase of the RF signal will be decelerated in the first acceleration gap and therefore be out of phase in the following gaps. This leads to a distribution of velocities that can be measured in our experiments. In the following we describe a simple 1D-model to calculate the measured beam currents.

III. 1D-MODEL OF THE RETARDING-FIELD ANALYZER

To interpret the ion current detected in the Faraday cup, we created a simple model to describe our experiment. For this model we assume a uniform ion beam profile of a given pulse length (long compared to the RF period). We then discretize the beam into N macro particle, evenly spaced along the z axis and assign a constant velocity to each macro particle. For each particle we track its energy, z-position, and time. We model the acceleration gaps as zero-length that provide instantaneous acceleration. Gap positions are calculated according to a given RF frequency, phase, amplitude, ion mass, and velocity. We also assume a single RF sine-wave with a fixed amplitude and frequency that applies to all RF gaps with no phase shifts, reasonable for the signal propagation time differences in the experiment. Then we trace each particle through the system by calculating the time it takes to arrive at the next gap, calculate the RF phase for that particle and add/subtract the RF voltage at that phase to the particles energy. All particles are tracked this way until they exit the last gap. At this point, the transmitted beam current is simulated by simply recording the macro-particles whose energy exceeds the grid voltage. The particles are then traced to the Faraday cup position where we can create a time histogram of the particles that can pass the retarding grid. This histogram can be scaled to present the measured beam current signal, as well as an average current. We implemented this algorithm in Python.

IV. EXPERIMENTAL RESULTS AND DISCUSSION

To demonstrate RF acceleration, we assembled two and three RF units and scanned the retarding-grid voltage for different RF amplitudes. In Fig. 3 we show the results of these measurements for the case of two RF units consisting of four acceleration gaps. The three measurements correspond to a high RF amplitude (300 mV driving voltage at the RF-signal generator), a medium amplitude (100 mV), and a low non-zero driving voltage (1 mV). This latter case was chosen (vs. powering off the electronics) to assure a well-defined voltage on the RF wafers for a "no-RF case". The details of the resulting voltage scan are shown in the inset of Fig. 3. This measurement verifies our incoming ion beam energy of 8 keV. Rather than a steep drop to zero over 0.5-2 eV (the expected plasma ion source temperature) the current falls over 10-15 eV. This apparent energy spread is not an attribute of the beam but instead it is likely due to the known lensing effect of the mesh and the associated contribution to the intrinsic FWHM sensitivity of the diagnostic. For our mesh (90 lines/inch, 5.5×10^{-3} inch rectangular mesh) the estimated FWHM energy resolution is 15 eV, according to the analytic model of Sakai and Katsumata [6].

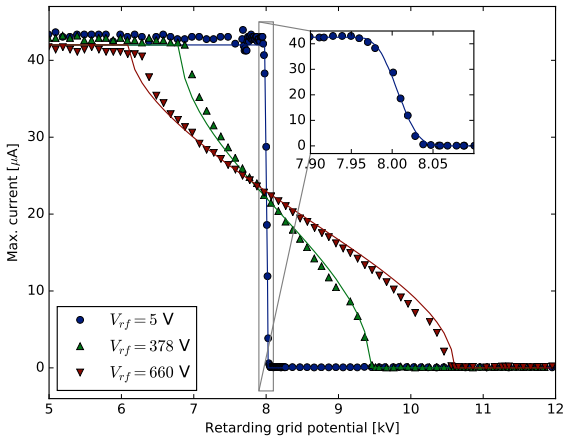

FIG. 3: Retarding-grid voltage scan with two RF units for low, medium and high RF voltages as described in the text. The inset shows a scan with the RF signal generator at its lowest setting. The simulations are shown as solid lines.

The solid lines in Fig. 3 show that simulation results using our 1D-model are in good agreement with the experiments. Note that the model has only one free parameters: the current level for low grid voltage settings. All other parameters, such as the gap distances, are taken from the experiment or measured directly, such as the RF frequency and RF amplitude (measured with a high voltage probe). To achieve a good match for the data shown in the inset of Fig. 3, we also assume a mesh resolution of 15 eV, which we implemented in the simulations by adding a gaussian distribution to the starting energy of the ions. The effect of an ion temperature would only be visible in the inset in Fig. 3, except that it is obscured by the 15 eV retarding-grid resolution. For the medium and high RF scans the ion temperature has a negligible effect on the results. The simulations therefore assume a monoenergetic beam.

In Fig. 4 results are shown from running three RF units (6 accelerations gaps). Since we are currently driving all RF gaps with a single circuit, we had to lower the frequency to get the best resonant condition in the circuit. The higher capacitance of the three RF unit compared to the two RF units also resulted in a lower voltage per

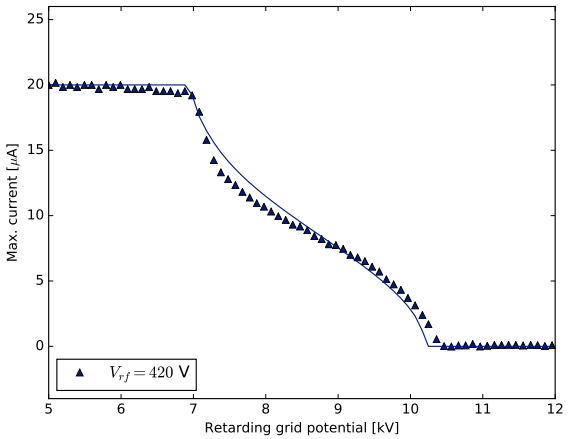

FIG. 4: Three RF units with an RF amplitude of 420 V and a frequency of 12 MHz.

wafer. Taking these effects into account, the results agree well with our simulations.

The extracted beam current from the source for these experiments is in both cases limited by the ion source conditions, which were optimized for stable source operation instead of high beam currents.

V. OUTLOOK

We showed the successful acceleration of ions using a compact RF structure based on FR-4. Ongoing experiments are integrating ESQs into the acceleration structure, as well as providing a six ESQ matching section between the ion source and the MEQALAC structure to be able to capture more ions from the source, reduce beam scraping and establish matched beam conditions at the entrance of the accelerator. In these experiments, the total acceleration is limited by the voltage that the RF amplification can supply. As a result, increasing the number of RF units did not appreciably increase the total acceleration because the larger load caused the voltage per acceleration gap to decrease. To be able to scale this technology to higher output voltages, by using more RF units with a higher acceleration gradient, we are working on integrating the RF generation on the wafer using coplanar waveguides and also on-chip RF generation. Using printed circuit boards enabled quick prototyping of devices. However, using laser cutting technology and FR-4 limits us to fabrication errors of $\sim 20\,\mu$m. Fabricating the wafers in silicon using standard optical lithography will reduce the fabrication error by another factor of 10. Allowing smaller beam apertures and therefore higher ion beam current. Lithography will also allow us to use large parallel arrays of beamlets and therefore increase the transported current.

We envision this technology to be applicable to beam energies between 100 keV to several MeV with beam current densities around $1\,{}^{\mathrm{mA}}/_{\mathrm{cm}^2}$ (when averaged over the total cross section of the accelerator structure of e.g. a 4" wafer). Applications areas range from material analysis to fusion drivers.

Acknowledgements

We are grateful for insightful discussions with Andris Faltens (LBNL). This work was supported by the Office of Science of the US Department of Energy through the ARPA-E ALPHA program under contract DE-AC0205CH11231 (LBNL).

[1] Ji, Q., Seidl, P.A., Waldron, W.L., Takakuwa, J.H., Friedman, A., Grote, D.P., Persaud, A., Barnard, J.J., Schenkel, T., 2016. Development and testing of a pulsed helium ion source for probing materials and warm dense matter studies. Review of Scientific Instruments 87, 02B707. URL: http://scitation.aip.org/content/aip/journal/rsi/87/2/10.1063/1.4932569, doi:http://dx.doi.org/10.1063/1.4932569.

[2] LabVIEW, . http://www.ni.com/labview/. [Online].

[3] Maschke, A., 1979. Space-charge limits for linear accelerators URL: http://www.osti.gov/scitech/servlets/purl/5914736, doi:10.2172/5914736.

[4] Persaud, A., Ji, Q., Feinberg, E., Seidl, P.A., Waldron, W.L., Schenkel, T., Lal, A., Vinayakumar, K.B., Ardanuc, S., Hammer, D.A., 2016. Ion acceleration in a scalable mems rf-structure for a compact linear accelerator. submitted arXiv:1610.09723.

[5] Python, . http://www.python.org. [Online].

[6] Sakai, Y., Katsumata, I., 1985. An energy resolution formula of a three plane grids retarding field energy analyzer. Japanese Journal of Applied Physics 24, 337. URL: http://stacks.iop.org/1347-4065/24/i=3R/a=337.

[7] Urbanus, W., Wojke, R., Bannenberg, J., Klein, H., Schempp, A., Thomae, R., Weis, T., Amersfoort, P.V., 1989. Meqalac: A 1-mev multichannel rf-accelerator for light ions. Nuclear Instruments and Methods in Physics Research Section B: Beam Interactions with Materials and Atoms 37, 508 – 511. URL: http://www.sciencedirect.com/science/article/pii/0168583X89902346, doi:http://dx.doi.org/10.1016/0168-583X(89)90234-6.

[8] ZeroMQ, . http://zeromq.org/. [Online].